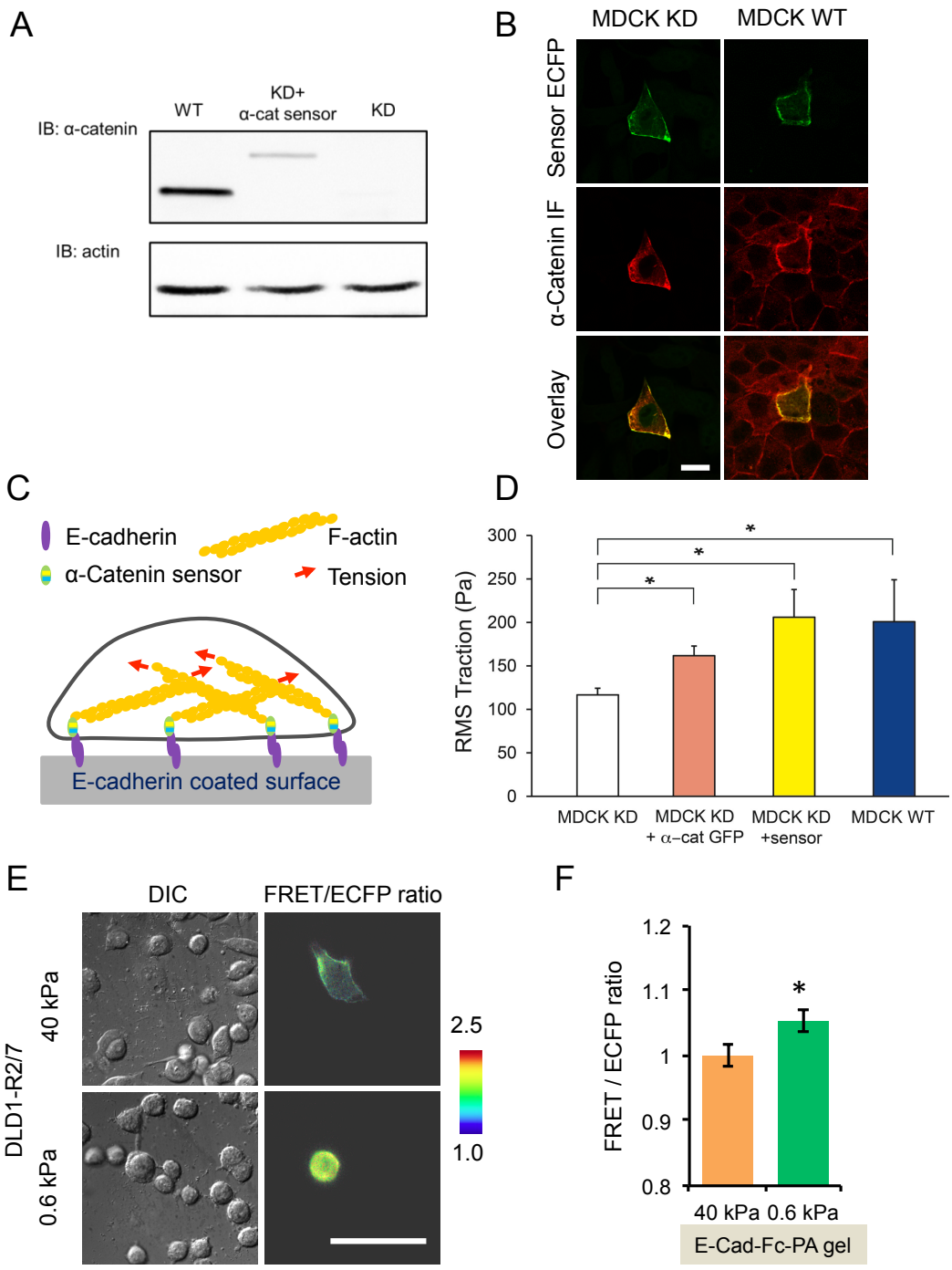

Figure S1 related to Figure 1. FRET-based α–catenin conformation sensor rescues spreading, traction force generation, and rigidity sensing at E-cadherin adhesions. **(A)** Western blot of WT α–catenin in MDCK WT and MDCK KD cells, and blot of the α–catenin

sensor transiently expressed in MDCK KD cells. The higher MW band (center lane) is the biosensor, with a MW equal to the size of WT α–catenin with inserted fluorescent proteins. The lower bands are actin-loading controls. **(B)** Fluorescence and immunofluorescence images of the α–catenin biosensor localization in MDCK KD cells (left) and in MDCK WT cells (right). The top panels are fluorescence images of the sensor expressed in both cell lines. The middle panels are IF images of α–catenin in MDCK KD and in MDCK WT cells. The bottom panels are the merged fluorescence and IF images showing that the sensor co-localizes with endogenous α–catenin at junctions. **(C)** Schematic of an E-cadherin-expressing cell adhering to a polyacrylamide gel coated with E-cadherin ectodomains. Actomyosin contractile forces in the cell generate traction forces on the substratum through specific E-cadherin adhesions. **(D)** The root mean square (RMS) traction forces (Pascal, Pa) generated by cells on E-Cadherin-Fc coated gels (34 kPa), in medium containing 0.5% FBS and anti-integrin antibodies. The cells were MDCK KD, MDCK KD cells expressing α–catenin-GFP, MDCK KD cells expressing the α–catenin sensor, and MDCK WT cells. The normalized traction force generated by the MDCK KD cells expressing the α-catenin sensor is statistically different from the MDCK KD cells (n=8, *P < 0.05), but statistically similar to MDCK WT cells (n=7, P = 0.93). **(E)** DIC and FRET/ECFP images of DLD1-R2/7 cells transiently transfected with the sensor and seeded on gels (40 kPa and 0.6 kPa moduli) covalently modified with canine E-Cadherin-Fc. The fluorescence images identify sensor-expressing cells in the population. Cells spread more on rigid (top) than on soft (bottom) gels. Scale bar = 10 μm. **(F)** FRET/ECFP ratios in DLD1-R2/7 cells expressing the biosensor and seeded on rigid (40kPa) and soft (0.6kPa) gels coated with E-cadherin. Immobilized E-Cad-Fc densities were similar on both gels [S1]. Increased traction forces on the rigid gel [S1] corresponded with lower FRET/ECFP ratios (n=24-28, *P<0.05). Error bars in panels C and F are the standard error of the mean (SEM).

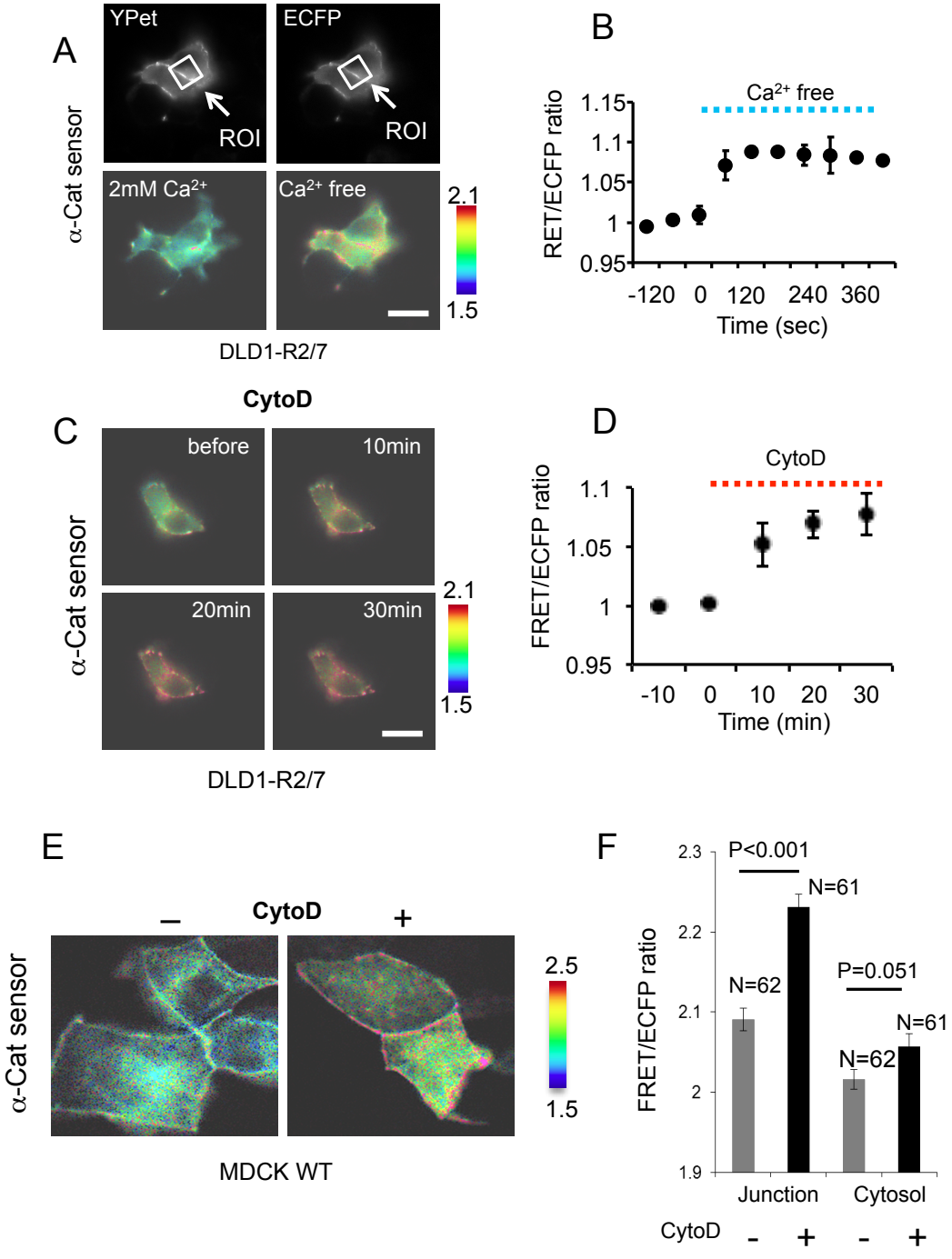

Figure S2 related to Figure 1. Changes in junction tension by cadherin inactivation or actin disruption alter the α-catenin sensor conformation. (A) FRET/ECFP ratios in ROIs (white squares) at junctions between DLD1-R2/7 cells transiently transfected with the sensor, in

response to cadherin inactivation by Ca^{2+} removal with medium containing 2mM EGTA. The upper panels show the YPet and ECFP fluorescence in the absence of Ca^{2+}. The lower panels show the FRET/ECFP ratios. In the presence of 2mM Ca^{2+} (left), the FRET/ECFP ratio is low (blue-green), but removing Ca^{2+} (right) increases the FRET/ECFP ratio at the junctions (green-red). **(B)** Time course of the FRET/ECFP ratio before and after Ca^{2+} removal, showing the rapid ~9% increase in the FRET/ECFP ratio in sensor-transfected DLD1-R2/7 cells (n=3). **(C)** FRET/ECFP ratio at indicated times after treating DLD1-R2/7 cells expressing the sensor with CytoD. Blue or green colors represent low FRET/ECFP (stretched conformation) and red indicates high FRET/ECFP (folded conformation). **(D)** FRET/ECFP ratio versus time before and after CytoD treatment (n=3). **(E)** FRET/ECFP images of MDCK WT cells expressing the sensor, before and 30 min after CytoD treatment. **(F)** Bar graph comparing FRET/ECFP ratios at ROIs at junctions between MDCK WT cells expressing the α-catenin sensor versus ROIs in the cytosol. Measurements were obtained before and 30min after CytoD treatment. Actin disruption increases FRET/ECFP ratios at junctions (Control vs. CytoD treatment; n=61-62, $P<0.001$), but only slightly in the cytosol (n= 61-62, $P=0.051$).

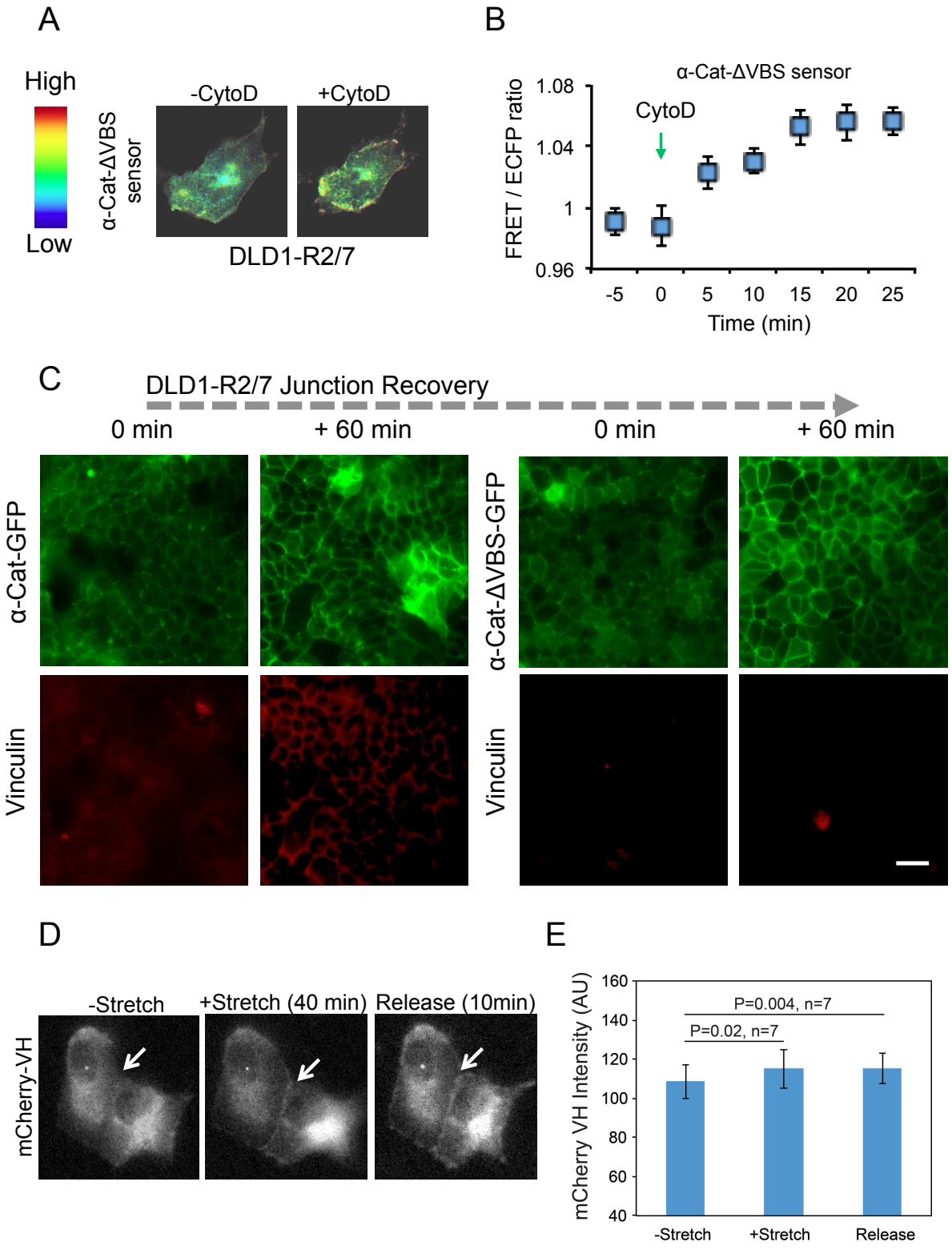
A
High
Low
α-Cat-ΔVBS sensor
-CytoD
+CytoD
DLD1-R2/7
B
α-Cat-ΔVBS sensor
CytoD
FRET / ECFP ratio
1.08
1.04
1
0.96
-5
0
5
10
15
20
25
Time (min)
C
DLD1-R2/7 Junction Recovery
0 min
+ 60 min
0 min
+ 60 min
α-Cat-GFP
Vinculin
α-Cat-ΔVBS-GFP
Vinculin
D
-Stretch
+Stretch (40 min)
Release (10min)
mCherry-VH
E
mCherry VH Intensity (AU)
160
140
120
100
80
60
40
P=0.004, n=7
P=0.02, n=7
-Stretch
+Stretch
Release

Figure S3 related to Figure 2 and Figure 4. Vinculin recruitment to intercellular junctions requires tension and the vinculin binding site of the α−Cat sensor. (A) FRET/ECFP images of a DLD1-R2/7 cell expressing the α−Cat-ΔVBS sensor before (left) and 30 min after (right) CytoD treatment. **(B)** Time-dependent FRET/ECFP ratio at junctions between DLD1-R2/7 cells transiently expressing the α−Cat-ΔVBS sensor, before and after CytoD addition (n=3). The α−Cat-ΔVBS sensor also undergoes a conformational change following actin depolymerization. **(C)** Vinculin and α−Cat-GFP (left) or vinculin and α−Cat-ΔVBS-GFP (right) localization at re-annealing junctions between DLD1-R2/7 cells, initially and 60min after Ca^{2+} addition. The top panels are GFP images of α−Cat-GFP (left) or α−Cat-ΔVBS-GFP (right) distributions, and the lower panels are immuno-fluorescence images of vinculin. **(D)** mCherry-VH localization at junctions between MDCK WT cell clusters before stretch, at 40min of stretch, and 10min after tension release. **(E)** Bar graphs of the mCherry VH intensity at junctions between MDCK WT cells before stretch, at 40min of stretch, and 10min after tension release (n=7).

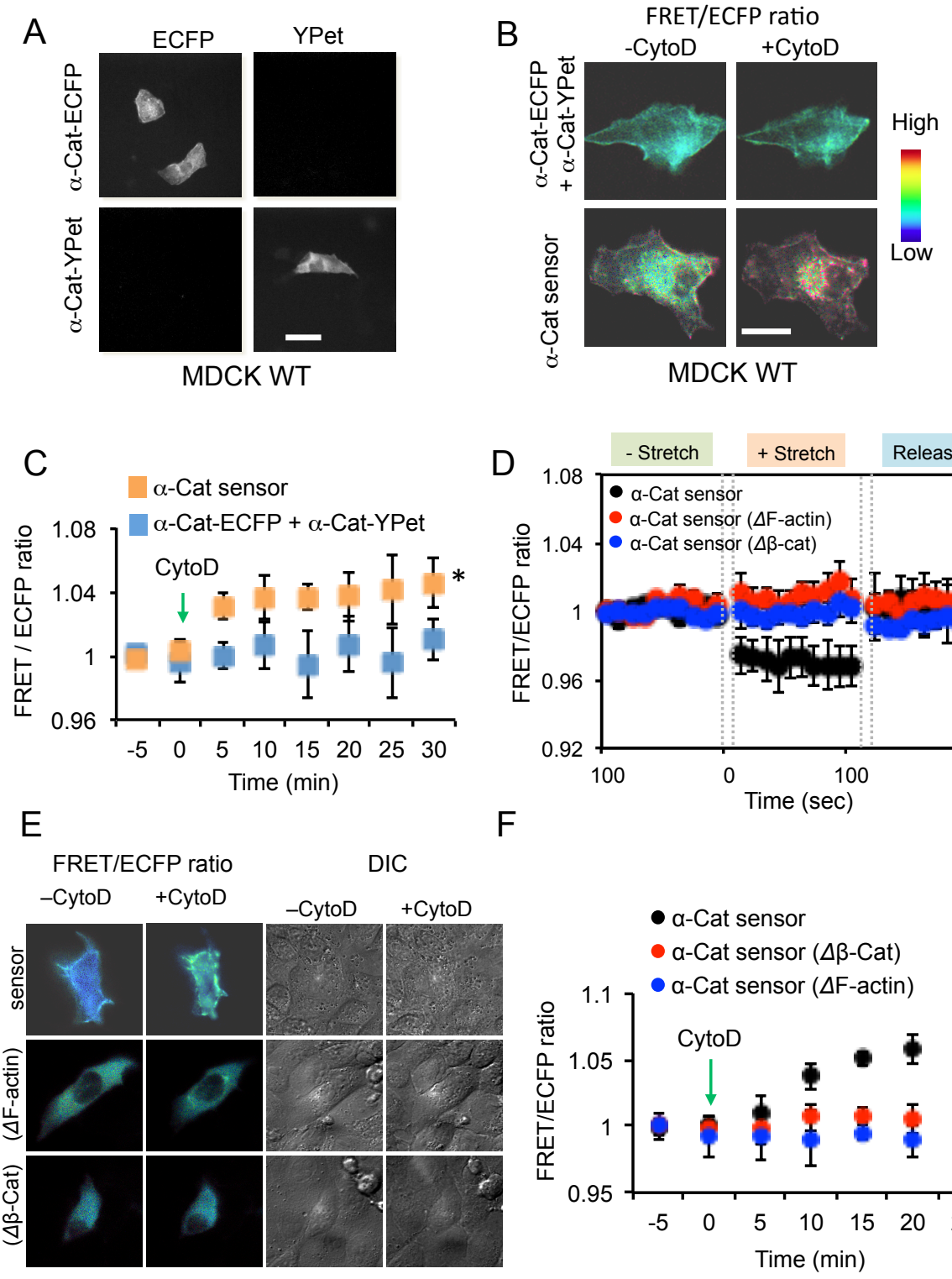
A
ECFP
YPet
α-Cat-ECFP
α-Cat-YPet
MDCK WT
B
FRET/ECFP ratio
-CytoD
+CytoD
α-Cat-ECFP + α-Cat-YPet
α-Cat sensor
High
Low
MDCK WT
C
α-Cat sensor
α-Cat-ECFP + α-Cat-YPet
CytoD
FRET / ECFP ratio
1.08
1.04
1
0.96
-5 0 5 10 15 20 25 30
Time (min)
*
D
- Stretch
+ Stretch
Release
α-Cat sensor
α-Cat sensor (ΔF-actin)
α-Cat sensor (Δβ-cat)
FRET/ECFP ratio
1.08
1.04
1
0.96
0.92
100 0 100 200
Time (sec)
E
FRET/ECFP ratio
DIC
–CytoD
+CytoD
–CytoD
+CytoD
α-Cat sensor
α-Cat (ΔF-actin)
α-Cat (Δβ-Cat)
F
α-Cat sensor
α-Cat sensor (Δβ-Cat)
α-Cat sensor (ΔF-actin)
CytoD
FRET/ECFP ratio
1.1
1.05
1
0.95
-5 0 5 10 15 20 25
Time (min)

Figure S4 related to Figure 1 and Figure 3. Effect of sensor mutations on FRET/ECFP changes following mechanical perturbations. (A) ECFP and YPet emission in MDCK WT cells transfected with either the α−Cat-ECFP or α−Cat-YPet sensor mutans in which YPet or ECFP fluorescence was quenched, respectively (see Fig. 1B). In cells transfected with α−Cat-ECFP (top) or with α−Cat-YPet (bottom), the YPet or ECFP fluorescence was quenched, respectively. In MDCK WT cells co-transfected with both mutants, the α−Cat-ECFP and α−Cat-YPet control sensors do not exhibit either YPet or ECFP fluorescence, respectively, upon excitation at 433 nm. Scale bar = 10 μm. **(B)** FRET/ECFP images of MDCK WT cells co-transfected either with both control sensors (top) or with the α-catenin sensor (bottom), before and 30 min after CytoD treatment. The co-transfected cells do not exhibit any change in FRET/ECFP, in contrast to the WT sensor. Scale bar = 10 μm. **(C)** FRET/ECFP versus time after Cyto D treatment of MDCK WT cells transfected with the WT α−Cat sensor (yellow squares) or co-transfected with the α−Cat-ECFP and α−Cat-YPet control sensors (blue squares). The control, co-transfected cells did not exhibit any significant FRET/ECFP change following CytoD treatment, whereas the WT α−Cat sensor FRET/ECFP ratio increased by ~4% (n=4-6, *P<0.05). Error bars are the SEM. **(D)** FRET/ECFP ratio with MDCK WT cells expressing the WT sensor or either of the ΔF-actin or Δβ-catenin truncation mutants, during a substrate stretch-release cycle with 10s intervals between stretch and imaging. During substrate stretching, the FRET/ECFP ratio between cells expressing the WT α−Cat sensor decreased abruptly by ~4% (n=6, *P< 0.05). After tension release, the FRET/ECFP ratio abruptly recoiled to the initial value prior to stretch. Neither the ΔF-actin nor the Δβ-catenin sensor mutant responded to substrate stretch, and the signals during stretch differed significantly relative to the WT α−Cat sensor (n=6, *p < 0.05). Error bars are the SEM. **(E)** FRET/ECFP (left) and DIC (right) images of MDCK KD cells expressing the α-catenin sensor or

either of the truncation mutants (ΔF-actin or Δβ-catenin), before and 30 min after CytoD treatment. **(F)** Time courses of the FRET/ECFP at junctions between transfected MDCK KD cells before and after CytoD treatment. There was a significant increase in the FRET/ECFP ratio in cells expressing the WT α-Cat sensor, in contrast to the two, truncation mutants (n=6, WT α-catenin sensor; n=6, ΔF-actin mutant; n=7, $\Delta\beta$-catenin mutant). Error bars indicate the SEM.

Supplemental Experimental Procedures

Sensor construction

The full-length human α-catenin cDNA in a pcDNA3 vector was from Addgene, Corp. (deposited by David Rimm), and was verified by sequencing. According to previous reports [S2, 3], there are three functional regions within the α-catenin protein: namely, the N-terminal aa22-264, central aa325-633, and the C-terminal aa671-906. The central domain comprises the postulated force sensitive region (Fig. 1A) that mediates α-catenin binding to different targets. Guided by prior studies and by functional mapping [S2], we inserted ECFP and YPet fluorescence proteins within flexible linker regions (aa265-324 and aa634-670) with the expectation that the construct would preserve α-catenin functions at cadherin adhesions, and that this construct would undergo postulated folding/unfolding changes that would in turn alter the energy transfer efficiency between these two fluorophores (Fig. 1A). Specifically, ECFP was inserted between G^{315} and A^{316} and YPet was inserted between D^{639} and D^{640} of the α-catenin sequence.

Vector NTI software identified restriction sites in the α-catenin mRNA sequence. To avoid cleaving the α-catenin cDNA sequence, we first generated five fragments that were linked with different restriction sites: (1) nucleotides 1-945 of α-catenin flanked by Nhe and Hind III; (2) the

ECFP cDNA flanked by Hind III and Kpn I sites; (3) nucleotides 946-1917 of α-catenin flanked by Kpn I and BamH I sites; (4) the YPet cDNA flanked by BamH I and EcoR I sites; (5) the remaining α-catenin cDNA (nucleotides 1918-2718) flanked by EcoR I and Not I. We then connected fragment 1 and 2 at the Hind III sites. Fragments 3 and 4 were coupled at BamH I, and the two fused sequences were then fused together via Kpn I. Finally, the fifth fragment was coupled to the C-terminus of the assembled fragments 1-4 via EcoR I, in order to complete the entire engineered α-catenin FRET biosensor. The construct was cloned into pcDNA3.1 for amplification, and then the construct was verified by sequencing.

ECFP and YPet were described previously [S4, 5]. The primers for each step are as follows. (1) For α-catenin fragment 1 (1-945), the sense primer is GCCTAGCTAGCATGACTGCTGTCCATGCAGGCAAC, and the anti-sense primer is GTCCCAAGCTTCCCACTAATGATGCTTTCCAGACGC. (2) For ECFP, the sense primer is ATGCAAGCTTATGGTGAGCAAGGGCGAGAGC, and the anti-sense primer is ATGC GGTACCGGCGGCGGTCACGAACTCCAG. (3) For the α-catenin fragment 3 (945-1917), the sense primer is ATGCGGTACCGCTGCCTTGATGGCCGACTCG, and the anti-sense primer is ATGCGGATCCATCCAACTCCTCAGGGGTCCTTA. (4) For YPet, the sense primer is TCGAGGATCCATGTCTAAAGGTGAAGAATTATTCAC, and the anti-sense primer is ATGCGAATTCTTTGTACAATTCATTCATACCCTCG. (5) For the C-terminal fragment of α-catenin (1918-2718), the sense primer is ATGC GAATTCGACTCTGACTTTGAGACAGAAGATT, and the anti-sense primer is ATGCGCGGCCGCT TAGATGCTGTCCATAGCTTTGAAC.

Sensor domain deletion mutants

Two α-catenin biosensor domain-deletion mutants were generated by PCR (Phusion DNA polymerase, NEB) and ligation (T4 DNA ligase, NEB). Deleting amino acid residues 48-

163 eliminated the β-catenin binding sequence (Δβ-cat mutant biosensor). PCR used the sense primer 5' TTGAGGAATGCTGGCAATGAACA 3' and an anti-sense 5' GGGCCCTTTACTATTGGTGTTTA 3'. Deleting amino acids 849-906 eliminated the F-actin binding site (ΔF-actin mutant). We used primers 5' TAAGCGGCCGCTCGAGTCTAG 3' and 5' CATACCCTGTGACTTTTGGTATTT 3'. The PCR products were phosphorylated by T4 Polynucleotide Kinase before ligation with T4 DNA ligase.

Site-Directed mutagenesis of fluorophores

Site directed mutagenesis was used to create two constructs that encoded either non-fluorescent ECFP or non-fluorescent YPet in the α-catenin sensor. A sense primer 5'CGTGACCACCCTGGCCGCGGGCGTGCAGTGC3' and an anti-sense primer 5'GCACTGCACGCCCGCGGCCAGGGTGGTCACG3 were used for the ECFP mutation. A sense primer 5' TGGCCAACCTTAGTCACTACTTTAGGTGCTGGTGGTCAATGTTTTG 3' and an anti-sense primer 5' CAAAACATTGAACACCAGCACCTAAAGTAGTGACTAAGGTTGGCCA 3' were used for the YPet mutation. With these primers, each α-catenin sensor with the mutation of ECFP (α-Cat-YPet) and of YPet (α-Cat-ECFP) were generated by PCR (Phusion DNA polymerase), and followed by with DpnI digestion for 1 hr at 37 °C.

Construction of the α-catenin ΔVBS sensor mutant

The α-catenin ΔVBS biosensor, lacking the vinculin-binding site (VBS) defined by amino acids 316-405 in α-catenin was engineered by substituting the native sequence with the homologous sequence from mouse vinculin (aa 514-606) [S2, 6]. First, an Age I site was introduced into the α-catenin biosensor (related to amino acids 406-407 of α-catenin) with a

QuikChange® Site-Directed Mutagenesis Kit (Stratagene). The mouse vinculin fragment (amino acids 514-606) was amplified by PCR with a sense primer containing a Kpn I site and a reverse primer containing an Age I site. Then the vinculin binding site in the sensor was excised by Age I and Kpn I digestion, and replaced with the homologous mouse vinculin fragment (aa 514-606).

Cell culture and chemicals

Studies used wild type Madin-Darby Canine Kidney cells (MDCK WT), and MDCK cells in which α-catenin has been stably knocked down (MDCK KD). The stable knock down of αE-catenin in MDCK cells was achieved with a hybrid vector kindly provided by Adam Kwiatkowski and James Nelson (Stanford University, Palo Alto, CA), as described [S7]. The vector contains an shRNA hairpin, which specifically targets canine αE-catenin [S8], pEGFP-C1, and the neomycin resistance gene for selection in G418 (400 μg/ml). Studies also used DLD1 cells and the DLD1-R2/7 line, which is a α-catenin null subclone of the DLD1 line.

The cells were cultured in Dulbecco's modified Eagle's medium (DMEM) supplemented with 10% fetal bovine serum (FBS), 2 mM L-glutamine, 1 unit/ml penicillin, 100 μg/ml streptomycin and 1 mM sodium pyruvate, except when indicated otherwise. Cells were maintained in 5% CO_2 in a humidified environment at 37 °C. DNA plasmids encoding the FRET sensor were transfected into the cells with Lipofectamine 2000 or LTX reagent (Invitrogen, Carlsbad, CA), according to the manufacturer's instructions. Cytochalasin D (Cyto D, 2 μM), ethylene glycol tetra acetic acid (EGTA, 2 mM), and gadolinium chloride ($GdCl_3$, 5 μM) were from Sigma. The hybridoma line producing the β1 integrin-blocking antibody, AIIB2 (used at 1:25 dilution of hybridoma culture medium), and the anti-integrin α6 antibody (GOH3, 20 μg/ml), and the anti-E-cadherin antibody (DECMA-1, 50 μg/ml) were from Santa Cruz Biotechnology

(Santa Cruz, CA). The neutral antibody (76D5 mAb, 10 μg/ml), which targets the E-cadherin extracellular domain [S9] was from Prof. B.M. Gumbiner. (University of Virginia).

Western Blot Analysis

Western blot analysis verified both the α-catenin knockdown in MDCK KD cells and the biosensor expression in both MDCK KD and MDCK WT cells. Cells were lysed with the Lysis Buffer (Cell Signaling Technology) containing 1 mM phenylmethanesulfonyl fluoride (PMSF, Sigma). The supernatant was clarified by centrifugation for 10 min at 20,800 g. To each sample, loading buffer was added containing 50 mM Tris-HCl, pH 6.8, 100 mM dithiothreitol, 2 % SDS, 0.01 % bromophenol blue, and 10 % glycerol. After heating at 95 °C for 5 min, the proteins were separated by SDS-PAGE, and then transferred to a nitrocellulose membrane. The membrane was incubated 5 w/v% nonfat milk in TTBS (10 mM Tris (pH 7.4), 150 mM NaCl, 0.05 % Tween-20) for 2 hr at room temperature. The membrane was incubated at 4°C overnight with rabbit, anti-α-catenin antibody (1:1000, Sigma) in TTBS containing 1 % BSA. After incubation, the membrane was washed three times with TTBS, incubated with horseradish peroxidase-conjugated anti-rabbit IgG (Santa Cruz, 1:2000) for 1 hr, and then quantified with an enhanced chemiluminescence system (Amersham, Arlington Heights, Ill., USA). As a loading control, the sample was also incubated at room temperature for 2 hr with a rabbit anti-actin antibody (1:1000, Sigma) in TTBS containing 1 % BSA.

Preparation of polyacrylamide gels and E-cadherin coating for traction force measurements

Polyacrylamide (PA) gels were cast on amino-silanized glass coverslips. First, 40% w/v acrylamide and 2% w/v bis-acrylamide stock solutions (Bio-Rad) were mixed in various

proportions to achieve different gel stiffness. The final concentrations of PA solution and bis-acrylamide crosslinker determined the gel moduli [S10]. To polymerize the solutions, 2.5 µl of 10% w/v ammonium persulfate (APS; Bio-Rad) and 0.25 µl of N,N,N9,N9-Tetramethylethylenediamine (TEMED; Bio-Rad) were added to yield a final volume of 500 µl PA solution. A photo active cross-linker, sulfo-SANPAH (0.5 mg/ml sulfosuccinimidyl 6-(4'-azide-2'-nitrophenyl-amino) hexanoate, Pierce, Rockford) was used to crosslink proteins onto the gel surface [S11, 12]. For adhesion via integrins, 200 µl of a 0.1 mg/ml fibronectin solution (from bovine plasma, Sigma) was incubated overnight with the PA gel at 37 °C.

To immobilize E-Cad-Fc on the PA gel, the Fcγ fragment of anti-human antibody (200 µg/ml) was chemically cross-linked to the polyacrylamide with sulfo-SANPAH (Pierce, Rockford, IL). Cross-linking reactions were carried out with the samples placed 15 cm beneath UV lamps. To modify glass coverslips, the Fcγ fragment was physisorbed, by incubation with the glass coverslip for 2 hr at room temperature. The antibody-modified substrates were washed with phosphate buffered saline (PBS), blocked with 10 % bovine serum albumin (BSA, Sigma) in PBS for 2 hr at room temperature, washed with PBS, and finally incubated overnight at 4 °C with purified canine E-Cad-Fc (10 µg/ml) in the presence of 1.8 mM $CaCl_2$ [S11].

The soluble, recombinant extracellular domain of canine E-cadherin with a C-terminal human IgG Fc tag (E-Cad-Fc) was purified from HEK293 cells that were stably transfected with a pcDNA3.1 plasmid encoding the E-Cad-Fc construct. Stable cells were maintained in DMEM with 10% FBS and G418 (400 µg/ml) [S13]. The protein was purified from cell culture medium by affinity chromatography (Affigel, BioRad), followed by gel filtration chromatography [S14].

Traction force and cell spreading measurements

In traction force measurements, cells were seeded at 2000-3000 cells/cm^2 on E-Cad-Fc-coated PA gels with embedded red fluorescent beads (0.2 μm, Molecular Probes, Eugene, OR) [S11]. The Young's moduli of the gels were 34 kPa [S11]. Cells were seeded on the gels for 6 hr, in medium containing 0.5% FBS (fetal bovine serum) and the anti-integrin antibodies GOH3 and AIIB2, in order to block integrin-mediated cell adhesion [S11]. The traction forces were determined using Fast Fourier Transform Software provided by N. Wang (UIUC) [S15]. Fluorescent images of the beads in the gel before and after trypsinizing the cells in Ca^{2+}-free medium (DMEM with 4.81mM EDTA) were captured, and bead displacements were used to calculate the root mean square traction forces with a custom MatLab program.

To measure cell spreading areas on E-cadherin substrata, DLD1-R2/7 cells transfected with α-catenin sensor were seeded on gels with moduli of 0.6 and 40 kPa, and then incubated overnight at 37 °C in DMEM containing 10% FBS and anti-integrin antibodies. Images were captured with a Zeiss Axiovert 200 inverted fluorescence microscope and analyzed by MetaFluor 6.2 and Image J software.

Nanoprobe substrate stretching assay

We used a nanoprobe tip to increase junctional tension, by exerting transverse strain in the hydrogel substrate supporting the cells. This new device for applying mechanical stretch to cell monolayers was previously described [S16]. Briefly, a glass probe tip was prepared with a micropipette puller, and then mounted on a small aluminum rod attached to a small, piezo XYZ positioning stage (Newport MT-XYZ model). The tip was accurately positioned above the gel with a larger XYZ linear stage (Newport 461 series), which pushes the probe tip around 20-25 μm into the gel, at a distance of ~30 μm from the cell boundary. Pulling the tip parallel to the gel applied tangential stretch to the substrate. After substrate stretching, the tip was detached from

the gel to release the substrate strain, and both the substrate and the attached cell monolayer relaxed back to the original position.

Cells were bathed in CO_2-independent medium (Gibco, Life technologies) while imaging cell junctions during the stretching cycles. To prevent medium evaporation, 1ml of Embryo tested sterile-filtered Mineral Oil (Sigma) was layered on top of the culture medium. An external heater was used to maintain temperature by providing warm air flow.

In the mechanical stretching experiment with mCherry-VH, images were captured every 5min for up to 40min with a Zeiss Axiovert 200 inverted fluorescence microscope. The mCherry fluorescence intensity (arbitrary units) in a ROI across the entire junction between two cells was analyzed by MetaFluor 6.2 and Image J software, after background subtraction. The intensities from three different images of the same cell junction, obtained at different time points during the stretching cycles (before stretching, ~40 min after stretching, and 10 min after release). Seven cell pairs were analyzed for statistical significance.

Junction recovery assay

FRET changes were monitored during junction assembly, following a Ca^{2+} switch. Briefly, a confluent monolayer of MDCK WT cells was washed once in low Ca^{2+} DMEM containing 5 μM $CaCl_2$, and then incubated with low Ca^{2+} medium containing 0.5% fetal bovine serum (FBS) for 30 min, in order to disrupt the cadherin junctions. The medium was then exchanged with DMEM containing 0.5% FBS and 2mM Ca^{2+}, which restored the adhesive function of E-cadherin. Line-scan analyses of regions of interest at intercellular junctions 1 hr after Ca^{2+} addition were performed with MetaMorph imaging software, in order to quantify changes in the fluorescence intensity during junction recovery. During the junction recovery, the vinculin intensity and the FRET/ECFP ratio were measured from immunofluorescence measurements at each time point.

In junction recovery measurements with cells transiently transfected with mCherry-Vinculin (mCherry-VN) constructs, cells were incubated with Ca^{2+} free HBSS (Hanks balanced salt solution, Invitrogen) for 15 min and then the medium was exchanged with DMEM containing 10% FBS and 2mM Ca^{2+} to activate junction re-annealing. Cherry fluorescence intensities at junctions were analyzed with Image J, MetaFluor 6.2 and MetaMorph software (Universal Imaging, West Chester, PA).

mCherry-Vinculin was made by exchanging EGFP with mCherry and mCherry-Vinculin 1-881 (mCherry-VH) was a kind gift from Dr. Johan de Rooij (Hubrecht Institute, University Medical Centre Utrecht) [S6]. MDCK WT cells were transiently transfected with these constructs using Lipofectamine.

To account for differences in expression within a population, data were averaged over cells with similar mCherry-VN (or mCherry-VH, 1-881) expression. To select the cell population for analysis, the distribution of fluorescence intensities (expression) was determined for several cells, and only cells within one standard deviation of the mean were further analyzed. The fluorescence in each cell was then background subtracted, and the mCherry fluorescence intensity in a ROI across the entire junction was determined before and at 15 min intervals after Ca^{2+} addition. The obtained, background-subtracted results with mCherry-VN were then validated against immunofluorescence measurements. Results with mCherry-VH were similarly obtained.

Kinetic rates were estimated from weighted, nonlinear least squares fits of the decay or recovery curves to pseudo first order rate equations (Kaleidagraph, Synergy Systems, Inc). The FRET/ECFP decay during junction recovery was fit to $A = A_0 \bullet \exp(-k_S t) + B$ where A_0 is initial FRET/ECFP signal, B is the limiting FRET/ECFP ratio and k_S is the rate of α–catenin stretching (DOF = 12). The mCherry accumulation kinetics was fit to $A = A_F (1-\exp(-k_A t))$ where A_F is the limiting accumulated mCherry VN (or mCherry VH) fluorescence and k_A is the accumulation rate

(DOF = 13). The rate constants are lumped parameters that convolve the junction re-annealing kinetics with the sensor stretching or vinculin binding kinetics. Because the junction re-annealing rates are the same when monitoring FRET/ECFP ratios or local vinculin accumulation, the kinetic differences reflect α–catenin-specific and vinculin-specific differences.

Combined magnetic twisting cytometry and FRET imaging

Carboxyl ferromagnetic beads (4.5 μm diameter, Spherotech, Lake Forest, IL) were covalently modified with E-cadherin-Fc or PLL (Sigma) [S17]. The beads were allowed to settle on the cell surfaces for 40 min at 37 °C and 5 % CO_2. Cells were gently rinsed to remove unattached beads, and then the glass-bottomed dish containing the cells was placed on a heated microscope stage. The beads were magnetized with a 1 Tesla pulse, and a 0.3 Hz oscillating magnetic field (70 Gauss) was applied orthogonal to the magnetization moment parallel to the cell for 2 min. This generated a continuously oscillating torque on the beads. While shearing attached beads with the MTC, dual-view FRET time course images were captured to monitor the change in the FRET/ECFP emission of the α-catenin sensor. Data were analyzed with a customized MatLab program. The region of interest (ROI) was selected near beads bound to cells, and the FRET/ECFP ratio was then calculated for each individual pixel that has been aligned and cross-correlated.

Immunostaining and Confocal Imaging

Confluent cell monolayers were washed three times with cold PBS, followed by fixation with 4 v/v% paraformaldehyde (Sigma) in PBS at room temperature for 15 min. After three washes with PBS, the samples were permeabilized with 0.1 % Triton X-100 in PBS for 30 min.

After permeabilization, the cells were blocked with 1 % BSA for 30 min at room temperature, washed with PBS, and then incubated for 2 hr at room temperature with a rabbit polyclonal anti-α-Catenin antibody (Sigma) or a monoclonal anti-Vinculin antibody (hVIN-1, Sigma) in PBS containing 1 % BSA. The secondary antibody, anti-rabbit IgG FITC or TRITC or anti-mouse IgG AlexaFluor 568 (Molecular Probes) prepared in PBS containing 1w/v% BSA, was incubated with the fixed cells for 1 hr at room temperature and then washed three times with PBS. Cells were mounted with ProLong Gold Anti-Fade (Invitrogen) and visualized with a Zeiss Axiovert 200 inverted fluorescence microscope. Confocal images were acquired on a Leica SP2 confocal laser scanning microscope with an x63/1.4 NA oil immersion objective and processed with Leica Software. For the α-catenin sensor and endogenous α-catenin, the 458 and 543 nm spectral lines from an argon-ion and helium–neon laser were used, respectively.

Time-Lapse Live-Cell Imaging

Live-cell fluorescent images were obtained with a Zeiss Axiovert 200 inverted microscope equipped with a charge-coupled device (CCD) camera (Cascade 512B, Photometrics), a 420DF20 excitation filter, a 450DRLP dichroic mirror, and two emission filters controlled by a filter changer (480DF30 for ECFP and 535DF25 for YPet). Time-lapse fluorescence images were acquired with MetaFluor 6.2 software (Universal Imaging, West Chester, PA). The emission ratios of YPet/ECFP (referred to as FRET/ECFP ratio) were directly computed and generated using MetaFluor software, and analyzed further with Excel (Microsoft, Redmond, WA). For the junction recovery assay, images were acquired with a Nikon fluorescence microscope with a Perfect Focus System (PFS), in order to maintain focus during junction assembly. MetaFluor 7.6 software was used to control the image acquisition and to analyze the fluorescence images. The filter used for ECFP imaging was 420/20 nm for

excitation and 480/40 nm for emission. The filters used for YFP imaging were 495/10 nm and 535/25 nm for excitation and emission, respectively.

To minimize the cell-cell heterogeneity, the baseline was first established, by averaging the FRET signals of each individual cell, before stimulation. This normalization process, which uses the established pre-stimulation base line for each cell, provides an internal normalization reference for the establishing the stimulation-dependent FRET changes of each cell. This approach reduces the cell-cell heterogeneity and noise. As such, although the overall response magnitude can be relatively small, the results are consistent across different cells because of this normalization procedure. This approach is described in several prior reports [S18-20].

The overexpression of the sensor does not affect the FRET signals because these two signals are not correlated within the range of our biosensor expression. This is mainly due to the innate design of the biosensor where a 1:1 ratio between the copy number of FRET donor and acceptor is maintained at any subcellular location [S5].

Supplemental References

S1. Tabdili, H., Barry, A., Langer, M., Chien, Y.-H., Shi, Q., Lee, K.J., Leckband, D. (2012). Cadherin point mutations alter cell sorting and modulate GTPase signaling. J Cell Sci *125*, 3299-3309.

S2. Yonemura, S., Wada, Y., Watanabe, T., Nagafuchi, A., and Shibata, M. (2010). alpha-Catenin as a tension transducer that induces adherens junction development. Nat Cell Biol *12*, 533-542.

S3. Shapiro, L., and Weis, W.I. (2009). Structure and Biochemistry of Cadherins and Catenins. Cold Spring Harbor Perspectives in Biology *1*, 1-22.

S4. Kim, T.J., Seong, J., Ouyang, M., Sun, J., Lu, S., Hong, J.P., Wang, N., and Wang, Y. (2009). Substrate rigidity regulates Ca2+ oscillation via RhoA pathway in stem cells. J Cell Physiol *218*, 285-293.

S5. Ouyang, M., Sun, J., Chien, S., and Wang, Y. (2008). Determination of hierarchical relationship of Src and Rac at subcellular locations with FRET biosensors. Proc Natl Acad Sci U S A *105*, 14353-14358.

S6. Twiss, F., le Duc, Q, vanderHorst, S, Tabdili, H, vanderKrogt, G, Wang, N, Rehmann, H, Huveneers, S, Leckband, D, de Rooij, J (2012). Vinculin-dependent cadherin mechanosensing regulates efficient epithelial barrier formation. Biol Open *submitted*.

S7. Benjamin, J.M., Kwiatkowski, A.V., Yang, C., Korobova, F., Pokutta, S., Svitkina, T., Weis, W.I., and Nelson, W.J. (2010). AlphaE-catenin regulates actin dynamics independently of cadherin-mediated cell-cell adhesion. J Cell Biol *189*, 339-352.

S8. Capaldo, C.T., and Macara, I.G. (2007). Depletion of E-cadherin disrupts establishment but not maintenance of cell junctions in Madin-Darby canine kidney epithelial cells. Mol Biol Cell *18*, 189-200.

S9. Petrova, Y.I., Spano, M.J., Gumbiner, B.M. (2012). Conformational epitopes at cadherin binding sites and p120-catenin phosphorylation regulate cell adhesion. Mol. Biol. Cell *in press*.

S10. Tse, J.R., and Engler, A.J. (2010). Preparation of hydrogel substrates with tunable mechanical properties. Current protocols in cell biology / editorial board, Juan S. Bonifacino ... [et al.] *Chapter 10*, Unit 10 16.

S11. Tabdili, H., Langer, M., Shi, Q., Poh, Y-C, Wang, N., Leckband, D. (2012). Cadherin-dependent mechanotransduction depends on ligand identity but not affinity. J Cell Sci *125*, 4362-4371.

S12. Barry, A.K., Tabdili, H., Muhamed, I., Wu, J., Shashikanth, N., Gomez, G.A., Yap, A.S., Gottardi, C.J., de Rooij, J., Wang, N., et al. (2014). alpha-Catenin cytomechanics: role in cadherin-dependent adhesion and mechanotransduction. J Cell Sci *127*, 1779-1791.

S13. Prakasam, A., Chien, Y.H., Maruthamuthu, V., and Leckband, D.E. (2006). Calcium site mutations in cadherin: impact on adhesion and evidence of cooperativity. Biochemistry *45*, 6930-6939.

S14. Sivasankar, S., Gumbiner, B., and Leckband, D. (2001). Direct measurements of multiple adhesive alignments and unbinding trajectories between cadherin extracellular domains. Biophys J *80*, 1758-1768.

S15. Butler, J.P., Tolic-Norrelykke, I.M., Fabry, B., and Fredberg, J.J. (2002). Traction fields, moments, and strain energy that cells exert on their surroundings. Am J Physiol Cell Physiol *282*, C595-605.

S16. Nishitani, W.S., Saif, T.A., and Wang, Y. (2011). Calcium signaling in live cells on elastic gels under mechanical vibration at subcellular levels. PloS one *6*, e26181.

S17. le Duc, Q., Shi, Q., Blonk, I., Sonnenberg, A., Wang, N., Leckband, D., and de Rooij, J. (2010). Vinculin potentiates E-cadherin mechanosensing and is recruited to actin-

anchored sites within adherens junctions in a MyosinII dependent manner. J Cell Biol *189*, 1107-1115.

S18. Lam, A.J., St-Pierre, F., Gong, Y., Marshall, J.D., Cranfill, P.J., Baird, M.A., McKeown, M.R., Wiedenmann, J., Davidson, M.W., Schnitzer, M.J., et al. (2012). Improving FRET dynamic range with bright green and red fluorescent proteins. Nat Methods *9*, 1005-1012.

S19. Gallegos, L.L., and Newton, A.C. (2011). Genetically encoded fluorescent reporters to visualize protein kinase C activation in live cells. Methods Mol Biol *756*, 295-310.

S20. Nezu, A., Tanimura, A., Morita, T., and Tojyo, Y. (2010). Visualization of Ins(1,4,5)P3 dynamics in living cells: two distinct pathways for Ins(1,4,5)P3 generation following mechanical stimulation of HSY-EA1 cells. J Cell Sci *123*, 2292-2298.